

# Identification of $\beta$ -meteoroids from measurements of the dust detector onboard the Ulysses spacecraft

A. Wehry and I. Mann

Max-Planck-Institut für Aeronomie, Max-Planck-Strasse 2, D-37191 Katlenburg-Lindau, Germany  
(e-mail: wehry@lindust.mpa.gwdg.de; mann@linmpi.mpg.de)

Received 25 May 1998 / Accepted 8 September 1998

**Abstract.** We investigate the detection of  $\beta$ -meteoroids (i.e. dust particles that leave the Solar system in unbound orbits from the direction of the Sun) in the data set of the Ulysses dust experiment. Analysis of the detection geometry of the experiment for the time span from launch until the end of 1995 shows that the detection of  $\beta$ -meteoroids is possible during 3 phases of the mission: in the first 100 days in the beginning of the mission in the ecliptic part of the orbit at heliocentric distances smaller than 1.6 AU, during the south polar passage, and at a time interval of approximately 150 days around the north polar passage. For these three intervals we can identify 48 particles in hyperbolic orbits with perihelion distances smaller than about 0.5 AU which may be classified as  $\beta$ -meteoroids. The mass distribution of the detected  $\beta$ -meteoroids covers a relatively small interval in the ecliptic path, but for the high latitude path it shows no significant difference from the mass distribution of other detected particles of presumably interplanetary origin. The flux of  $\beta$ -meteoroids derived from the data amounts to  $1.5 \pm 0.3 \cdot 10^{-4} m^{-2} s^{-1}$  between 1.0 and 1.6 AU in the ecliptic plane, and amounts to  $9.0 \pm 6.3 \cdot 10^{-5} m^{-2} s^{-1}$  between 1.8 and 2.7 AU at solar ecliptic latitudes between  $67^\circ$  and  $79^\circ$  during the north polar passage.

**Key words:** interplanetary medium – meteoroids

## 1. Introduction

The in-situ detection of  $\beta$ -meteoroids, i.e. dust particles in hyperbolic orbits away from the Sun has been reported for the first time by Berg & Grün (1973) and by Zook & Berg (1975), based on measurements of the Pioneer 8 and 9 spacecraft. Grün & Zook (1980) invented the expression  $\beta$ -meteoroid, as opposed to the so called  $\alpha$ -meteoroids, which are particles that were detected to come from the apex direction of the spacecraft. They determined the flux of  $\beta$ -meteoroids at 1 AU to be  $8.2 \cdot 10^{-4} m^{-2} s^{-1} (2\pi sr)^{-1}$  for particles of masses  $\leq 10^{-12} g$  (Berg & Grün, 1973). A flux of  $\beta$ -meteoroids has also been identified in the data of the micrometeoroid detector onboard Helios 1 at solar distances between 0.31 and 0.98 AU in the ecliptic (Grün et al., 1980).

The existence of particles that escape from the Solar system in hyperbolic orbits, is known for the surrounding of comets. Particles are ejected from the Solar system in unbound orbits when the repelling force from the solar radiation is of the same order of magnitude as solar gravity. The orbital parameters for the released particle depend on the exact conditions at the time of the dust ejection from the comet (see for instance Krésak, 1976). The orbital elements of the parent body as well as the acting radiation pressure force determine the orbit of the released particle. The detection of  $\beta$ -meteoroids points to the fact that a similar process must occur near the Sun. Dust particles in unbound orbits can be produced in the case of mutual collisions of micrometeoroids and larger meteoroids, as well as from the sublimation of dust particles near the Sun (cf. Mukai, 1985, 1996; Schwehm, 1977). Mukai (1996) has shown that absorbing particles may be forced into orbits of higher eccentricity when their size is reduced by sublimation and radiation pressure force increases. Also a collisional evolution of dust particles is expected to take place in the interplanetary dust cloud inside 1 AU (Leinert et al., 1983; Grün et al., 1985) as well as very close to the Sun (Ishimoto & Mann, 1996).

Since the study of  $\beta$ -meteoroids will reveal their possible formation process it helps towards a better understanding of the mass balance and collisional evolution of the interplanetary dust cloud. We will investigate the detection of  $\beta$ -meteoroids from the measurements of the dust experiment onboard ULYSSES (Grün et al., 1992a). As was shown in a previous study by Baguhl (1993), the Ulysses dust detector has detected  $\beta$ -meteoroids during the first phase of the mission 1990–1992 in its ecliptic orbit from 1 to 1.6 AU. We now check for a possible detection of  $\beta$ -meteoroids at high ecliptic latitudes. Our analysis is based on the data set which is published in the Ulysses/Galileo data page (Grün et al., 1995a) including measurements up to the end of 1995 which covers both passages of the solar poles. Using some basic assumptions we will develop a method to describe the orbits of  $\beta$ -meteoroids that could cross the Ulysses orbit. We calculate the detection probabilities for these possible fluxes of  $\beta$ -meteoroids for the detection geometry of the dust detector on the Ulysses-spacecraft (Grün et al., 1995b), and compare them to the earlier study by Baguhl (1993). Applying this method to the data set, we derive the flux rate of  $\beta$ -meteoroids for the eclip-

tic and for the out-of-ecliptic part of the Ulysses orbit and we estimate the orbital parameters of the identified  $\beta$ -meteoroids.

## 2. Ulysses impact data

The Ulysses spacecraft was launched in October 1990 and after its passage through the asteroid belt it was deflected in an out-of-ecliptic orbit during a flyby at Jupiter. This orbit is nearly perpendicular to the ecliptic plane and passes through the regions above the solar poles (Wenzel et al., 1992). The different stages of the mission are the southern polar passage at a distance of 2.3 AU in August 1994, the crossing of the ecliptic plane at 1.3 AU in February 1995 and the passage of the northern solar pole in the time span of June to September 1995 at a distance of about 2.2 AU. Data from the dust detector are studied until December 1995, when the spacecraft was at 3.0 AU and  $62^\circ$  ecliptic latitude (Grün et al. 1997; Krüger et al., 1998).

The dust detector is a multi-coincidence impact ionisation detector which measures submicrometer- and micrometer-sized dust particles. A detailed description is given by Grün et al. (1992a, 1992b). The detector has a geometric area of  $0.10m^2$ . It is mounted  $85^\circ$  to the spin axis of the spacecraft which is pointing towards the Earth. This determines the detection geometry of the dust detector. The experiment measures particles in the mass range from  $10^{-16}$  to  $10^{-6}$  g with impact speeds from 2 to 70 km/s (Grün et al., 1992b). The uncertainty in the speed determination amounts to a factor of 1.6 and the mass of impacting particles is determined to a factor of 6. The experiment detects particles within a viewing cone of  $140^\circ$  relative to the sensor axis which yields a limit to the determination of the impact direction and hence to the determination of the orbital parameters of the detected grains (Grün et al., 1995a, 1995b).

Essentially three different components of dust were so far identified in the data. Streams of particles were detected during the time before and after the Jupiter encounter. These streams are limited to a mass interval from  $10^{-15}$  to  $10^{-14}$  g and they come from the Jovian environment (Grün et al., 1993). Particles that enter the solar system from interstellar space have been identified in the data from their high impact speed and from their impact directions (Grün et al., 1994). The latter are comparable to the direction of the interstellar neutral gas flux measured onboard the same spacecraft (Witte et al., 1993). The remaining set of dust impacts may be assumed to be interplanetary dust particles. This is especially the case for the ecliptic path of the mission. The particles of this latter component tend to have relatively high impact velocities and the masses are typically lower than the mass of the particles that were classified as interstellar. Hence  $\beta$ -meteoroids, as well as particles that were ejected by Lorentz-forces and also interstellar particles that were depleted from their original flux direction may contribute to this component. In our study we work with this latter “interplanetary” component. We will use the data set after excluding the time period where the Jupiter streams have been detected and after subtracting impacts that are classified as interstellar according to the criteria given by Baguhl et al. (1994), i.e. from their impact velocity and mass.

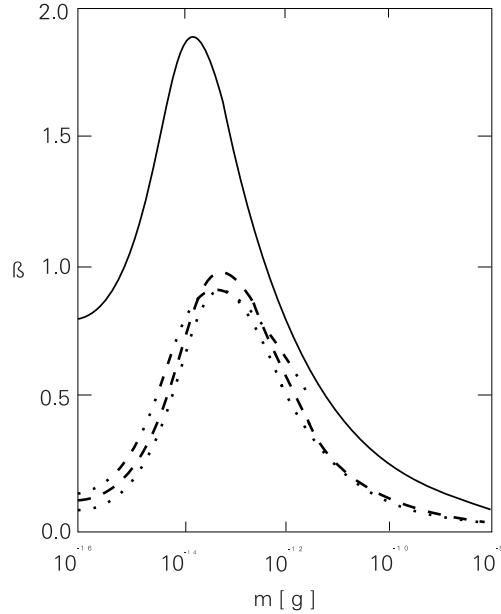


**Fig. 1.** The ratio,  $\beta$  of radiation pressure force and gravity force as a function of particle mass for different dust models. Solid line: young cometary; dotted line: old cometary; dashed line: asteroidal; dash-dotted line: interstellar particles (Wilck & Mann, 1996)

## 3. Dust orbits and detection probabilities

### 3.1. Dust orbits

In general interplanetary particles are moving on Keplerian orbits around the Sun under the influence of the solar gravitational attraction. The radiation pressure force  $F_r$  counterbalances the gravitational force  $F_g$  to an effective force:  $F_{eff} = F_g + F_r$ . The  $\beta$ -value is defined as the ratio of radiation pressure  $F_r$  to gravity  $F_g$  and leads to  $F_{eff} = (1 - \beta) \cdot F_g$ . The velocity of a particle in a circular orbit in this photo-gravitational field (cf. Baguhl, 1993) is  $v = \sqrt{\frac{\mu}{(1-\beta) \cdot r}}$ , where  $v$  is the Keplerian velocity,  $\mu$  is the reduced mass and  $r$  is the solar distance.

The velocity which is needed to keep a particle in a circular orbit, or more generally in a bound elliptic orbit, decreases with increasing  $\beta$ -value. Compared to the case when only gravity applies, the velocity is reduced by the factor  $\sqrt{1 - \beta}$ . Since this is also the case for the escape velocity, particles with high  $\beta$ -values will be in unbound orbits. When the reduction in size of a given particle leads to a higher  $\beta$ -value, it will, with the same velocity, consequently be in a more elliptic, respectively hyperbolic orbit.

The  $\beta$ -value is independent of the solar distance  $r$  and depends on the physical properties, i.e. on the mass, material, composition and structure, as well as the size of dust particles. Fig. 1 shows the mass dependency of the  $\beta$ -value for different particles (see Wilck & Mann, 1996). For particles of given optical properties the  $\beta$ -value has a maximum at about  $10^{-14}$ – $10^{-13}$  g so that it is likely that particles in this mass range are more easily launched into unbound orbits than particles of a different mass. This mass range corresponds to particle radii between 0.1 and

0.2  $\mu\text{m}$  assuming a bulk density of about  $3 \text{ g cm}^{-3}$  for the dust (cf. Leinert & Grün, 1990).

If  $\beta$ -meteoroids are detected at large distances from their perihelion, they move nearly radially outward and can easily be identified from their flux direction. The radial flux direction together with the velocity would also allow us to derive the probability that the particles are detected with the Ulysses dust experiment. We make an estimate as to which extent the flux of  $\beta$ -meteoroids can be described as radial at the position of the spacecraft. We are assuming parent bodies ( $\beta = 0$ ) moving in Keplerian orbits of a given eccentricity,  $e$  and perihelion distance,  $q$  which release a smaller particle due to either fragmentation or sublimation. For the Keplerian motion of a particle in the photo-gravitational field the velocity in the heliocentric system is given as

$$v^2 = \mu(1 - \beta) \left( \frac{2}{r} \pm \frac{e - 1}{q} \right) \quad (1)$$

(+ for  $\beta < 1$  and – for  $\beta > 1$ ).

We assume that these particles are produced from bigger particles in the perihelia of their Keplerian orbits. We do not take into account the mechanism, how the particles are formed, i.e. whether sublimation or collisions of parent bodies are responsible for the origin of these  $\beta$ -meteoroids. The particles maintain their perihelion velocities, which, due to the reduced potential (or reduced attracting force), leads to a less bound, or even hyperbolic orbit.

Assuming the perihelion velocity of the fragment to be the same as the velocity of its parent body the semi-major axis,  $a'$  of the newly formed particle can be written as

$$a' = a_0 \frac{1 - \beta}{1 - 2\beta \frac{a_0}{r_0}}, \quad (2)$$

using the indices 0 for the orbital elements of the parent body (see for instance Krésak, 1976).

We derive a set of possible orbits of  $\beta$ -meteoroids by assuming different solar distances of their formation, different  $\beta$ -values, and different eccentricities for the orbits of the parent body. We then determine the velocity and the radial velocity component as a function of the solar distance,  $r$ .

Table 1 gives the eccentricity and the perihelion distance of the orbit of the parent body and the assumed  $\beta$ -value of the fragment. This  $\beta$ -value is the lowest possible value, so that the new particle will be in an unbound orbit. From that we derive the parameters of the orbit at a distance of 2.5 AU from the Sun in the two right columns of the table. Assuming, in the first line, a circular orbit of the parent body at 0.3 AU and a  $\beta$ -value of 0.5 the velocity of the new particle is 19 km/s at 2.5 AU and the direction differs by  $14^\circ$  from the radial direction. Comparing this  $14^\circ$  to the detection cone of the experiment, which amounts to  $140^\circ$ , such a flux of particles can be assumed as directed radially outward. The same is the case for particles with higher  $\beta$ -values or for particles with higher perihelion velocities, when already the parent bodies have non circular orbits. From that we can conclude that  $\beta$ -meteoroids which are formed inside 0.3 AU

**Table 1.**

$e_0$	$q(\text{AU})$	$\beta$	$\gamma(^{\circ})$	$v(\frac{\text{km}}{\text{s}})$
			2.5 AU	2.5 AU
0	0.3	0.5	14	19
	0.8	0.5	24	19
0.3	0.3	0.4	11	27
	0.8	0.4	21	27
0.6	0.3	0.2	14	24
	0.8	0.2	24	24
0.9	0.3	0.2	9	38
	0.8	0.2	19	38

$e_0$	Eccentricity of the parent body
$q$	Perihelion distance
$\gamma$	Angle between the Solar direction and the particle velocity
$v$	Speed

around the Sun with  $\beta$ -values  $> 0.5$  would produce a nearly radial flux of particles at the position of the spacecraft. Assuming the model calculations by Wilck & Mann (1996) for  $\beta$ -values of typical interplanetary dust,  $\beta$ -values  $> 0.5$  would occur in the mass range from  $10^{-15}$  to  $10^{-12}$  g based on their model assumptions for asteroidal dust particles and in the mass range from  $10^{-16}$  to  $10^{-11}$  g based on their assumptions for young cometary dust particles. At this point we should note that our estimate does not include assumptions about the relative velocities between the parent body and the fragment. However, this can be expected to be small compared to the orbital velocities (see Ishimoto & Mann, 1996). The estimate for a parent body in a non-circular orbits would also change slightly, if the fragmentation of the parent body is not in the perihelion of the orbit.

### 3.2. Detection probabilities

To answer the question, “when is it possible to detect a radial flux of particles coming with different velocities from the Sun?”, we determine the relative velocities between the particle and the spacecraft. We derive the angle between the velocity vector of the dust particle relative to the spacecraft and the spin axis of the spacecraft along its orbit. From that we derive the effective detection area of the dust detector for a radial flux of particles and finally the detection probability as a function of time.

The effective detection area of the dust detector, which is averaged over a spin period (approximately 5 revolutions per minute), is a function of the angle between the impact direction and the spin axis. For a directed dust flux the maximum sensor area for particles with an impact direction parallel to the symmetry axis of the detector amounts to  $0.02 \text{ m}^2$  (Grün et al., 1992a). It is lower for other impact directions. We derive the effective detection area and identify the time spans, in which  $\beta$ -meteoroids could be detected. This “effective area” was first mentioned by Wilck (1994) and used to estimate detection probabilities for dust fluxes of different orbital parameters. We calculate the effective area of the detector for particles that

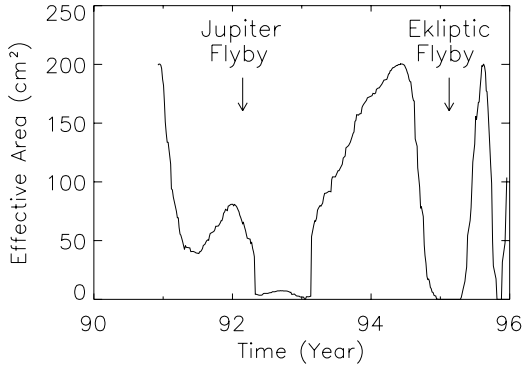


**Fig. 2.** The effective detection area of the dust experiment for particles incoming from the radial solar direction is shown as a function of time. This area is high in 1991 directly after launch and again shortly before and after the flyby through the ecliptic plane.

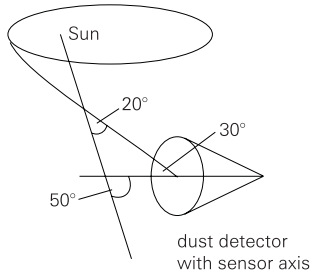


**Fig. 3.** Geometry of the dust detector: we assume that particles can be identified as  $\beta$ -meteoroids, if the angle between the Sun and the sensor axis of the detector at the time of the impact event is less than about  $50^\circ$ . This value results on the one hand from the model calculation ( $20^\circ$ ) mentioned in the text and on the other hand from the geometry of the detector ( $30^\circ$ ).

stream radially from the Sun. This calculation is made along the orbit of the spacecraft. The effective area is shown in Fig. 2 as a function of time. The described effective area was high in 1991 directly after launch, i.e. there was a high detection probability for  $\beta$ -meteoroids. A high detection probability for  $\beta$ -meteoroids occurred again in 1994 and 1995 shortly before and after the passage through the ecliptic plane. The effective area, however, is always below 20% of the geometric area of the detector, i.e.  $\beta$ -meteoroids always have a low detection probability. This is a result of the geometry of the dust experiment which, due to experimental reasons, never directly faces the Sun.

#### 4. Detection probability

We check the data set for the time intervals of the mission in which  $\beta$ -meteoroids could be detected applying the following criteria for  $\beta$ -meteoroids. Because there is no information about the exact impact direction of the particles available we assume an impact perpendicular to the surface of the detector (i.e. anti-parallel to the sensor axis). We take the impact direction to vary for  $30^\circ$  from the nominal direction perpendicular onto the detector. In comparison to the detection probability as a function of impact angle this would account for 50% of all detected particles in the case of an isotropic flux (Grün et al., 1992a). From the

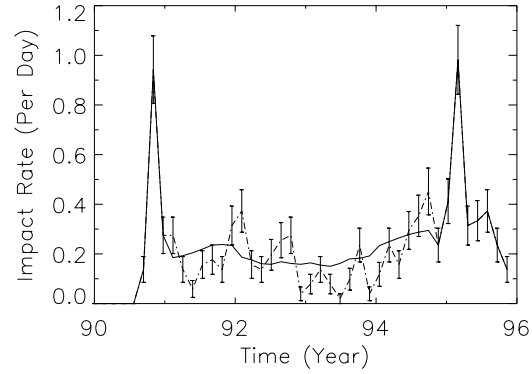


**Fig. 4.** The impact rate is shown against the time of impact. The rate is averaged over 50 days. The error bars are calculated with the gaussian statistics. The solid line shows a smoothed curve through the data.

model calculation we assume a maximum angle of  $20^\circ$  between the direction of the particle velocity and the radial direction in order to take into account that the flux of the particles still varies from the radial direction as mentioned before. According to this estimate the measured particles can be  $\beta$ -meteoroids, if the angle between the Sun and the sensor axis is less than about  $50^\circ$  at the time of the impact. Furthermore, from the model calculation identified  $\beta$ -meteoroids particle velocities have to be larger than 20 km/s (at heliocentric distances greater than 1.8 AU, which is the case for the time intervals 2 and 3 in our study) and larger than 30 km/s closer to the Sun at heliocentric distances smaller than 1.6 AU (i.e. in the first time interval according to Fig. 2).

#### 5. $\beta$ -meteoroids inside and outside the ecliptic

Looking at the set of detected interplanetary particles we try to obtain some direct indication from the data in order to predict  $\beta$ -meteoroids. This is done with the help of the impact rate as well as with the help of the distribution of the rotation angle of the spacecraft at the time of the impact. (For the definition of rotation angle see Grün et al, 1993). Fig. 4 shows the impact rate averaged over 50 days together with the error bars based on the Gaussian statistics whereas the solid line represents the smoothing curve. During the first weeks of measurements within the ecliptic we see a high impact rate which may be due to the detection of  $\beta$ -meteoroids. In the out-of-ecliptic part of the orbit a slightly increasing impact rate can be observed in the second part of the year 1995 shortly after the large increase of impact rate during the ecliptic passage, an indication that  $\beta$ -meteoroids are detected in addition to the usual flux rate. There is no obvious increase of the flux rate in the southern hemisphere.

On the basis of the maximum deviation from the solar direction together with the minimum speed condition described before we can identify 25  $\beta$ -meteoroids in the first part of the orbit within the ecliptic, 4  $\beta$ -meteoroids in the southern interval and 19  $\beta$ -meteoroids in the interval of the orbit north from the ecliptic plane.

The first time span can be compared with results from Baguhl (1993). He assumed the mass of particles and the rotation angle of the detector at the time of impact as a criterion

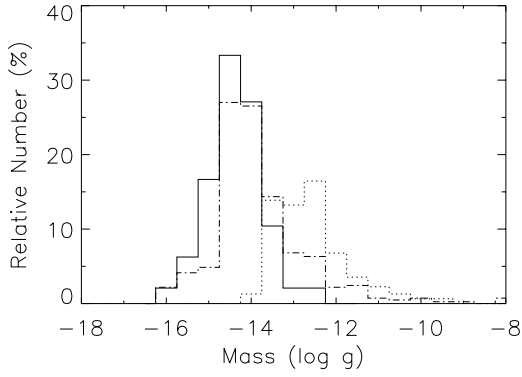


**Fig. 5.** The mass distribution of  $\beta$ -meteoroids is given in comparison to the mass distribution of the interstellar and interplanetary component (solid line:  $\beta$ -meteoroids, dotted line: interstellar component, dashed-dotted line: interplanetary component).

for  $\beta$ -meteoroids. Particles identified as  $\beta$ -meteoroids in this part of the mission are in a small mass interval from  $10^{-15}$  to  $10^{-13}$  g compared to the total mass interval of the detected particles between  $10^{-16}$  and  $10^{-8}$  g. This means that  $\beta$ -meteoroids are detected in a mass range where particles can have high  $\beta$ -values. Both the distributions of the particle mass as well as the distribution of the detector rotation angle for the impacts that we identified as  $\beta$ -meteoroids confirm the criteria that Baguhl used in his analysis.

In Fig. 5 the mass distribution of the  $\beta$ -meteoroids identified within the ecliptic as well as in the out-of-ecliptic part is presented in comparison to the mass distribution of the interstellar and interplanetary component. In contrast to the interstellar component there is no big difference between the distribution of the  $\beta$ -meteoroids and the mass distribution of the remaining interplanetary particles. A more careful study of this difference shows that the mass distribution of these  $\beta$ -meteoroids is slightly shifted to smaller particles. The mass values of the particles detected in the out-of-ecliptic part of the mission tend to be higher. While the number of  $\beta$ -meteoroids within the ecliptic and within the northern polar passage corresponds nearly to 25 per cent of the detected number of the interplanetary particles at this point of the orbit, the  $\beta$ -meteoroids amount only to about 5% of the detected particles within the southern hemisphere. For the latter part the mass values of  $\beta$ -meteoroids are slightly higher than in the other mentioned parts.

Together with the velocity and the position of the spacecraft we calculate the orbital elements especially the perihelion distances of detected  $\beta$ -meteoroids in order to find their place of origin. We assume that the particles reach the detector perpendicularly, i.e. the impact velocity vector is antiparallel to the sensor axis. The uncertainty in the speed determination mentioned above leads to an error area shown in Fig. 6, where the perihelion distances are presented within the ecliptic as well as for the out-of-ecliptic part. Regarding the part within the ecliptic we can conclude the origin of detected  $\beta$ -meteoroids to be inside 0.5 AU around the Sun.

For a better determination of the orbital parameters, we, a priori, assume that the particles that were classified as  $\beta$ -

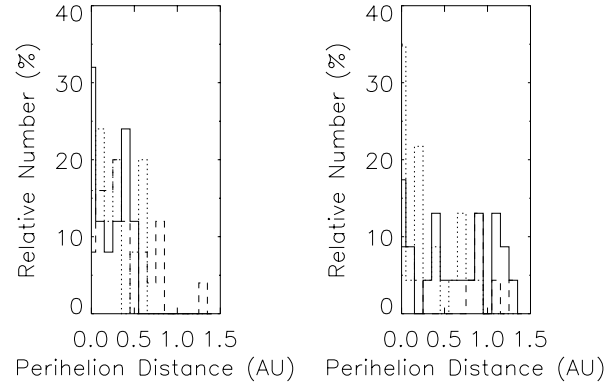


**Fig. 6.** The perihelion distances of detected  $\beta$ -meteoroids are calculated under the assumption that the particles reach the detector perpendicularly. The uncertainty in the speed determination leads to an error area. *Left side:* perihelion distance for  $\beta$ -meteoroids detected within the ecliptic; *right side:* perihelion distance for  $\beta$ -meteoroids detected in the out-of-ecliptic part.

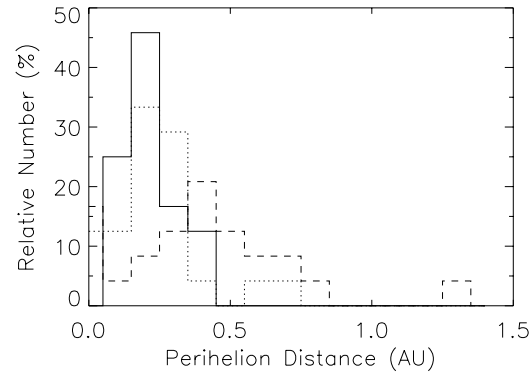


**Fig. 7.** The distribution of the corrected perihelion distances for the out-of-ecliptic part is given including the uncertainty in the speed determination. This correction assumes that particles hit only the part of the opening cone, which turns to the Sun.

meteoroids impact only the part of the opening cone, which turns to the Sun. Based on this restricted detection area we determine the perihelion distances of orbits. The resulting distribution for the averaged perihelion distances including the uncertainty in the speed determination shows values smaller than about 0.5 AU, as shown in Fig. 7. However due to the large number of assumptions the distribution should be seen rather as an indication than as a clear experimental result.

## 6. Flux of $\beta$ -meteoroids

We determine the flux of  $\beta$ -meteoroids according to the following equation:

$$F(t) = \frac{1}{\Delta t} \int_t^{t+\Delta t} \frac{N(t')}{A(t')} dt', \quad (3)$$

where  $\Delta t$  represents the time interval of the measurement,  $A$  is the effective area of the detector in this time interval and  $N$  stands for the number of particles detected within the interval  $[t', t' + dt']$ .

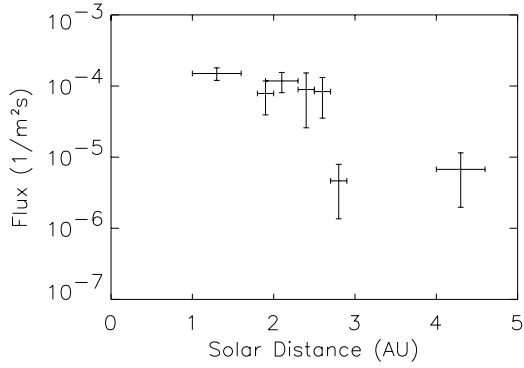


**Fig. 8.** The flux of  $\beta$ -meteoroids that is derived from the impact data presented as a function of the solar distance. The observed flux indicates a decrease to larger solar distances.

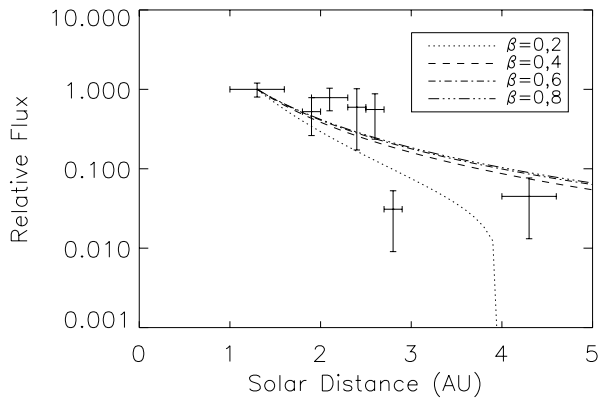


**Fig. 9.** Flux rates for different orbital parameters (here: eccentricity of the parent body  $e_0 = 0.4$ , perihelion distance  $q_0 = 0.5$  AU) are calculated in relation to the flux rate near 1 AU (small dashed line:  $\beta = 0.2$ , dashed-dotted line:  $\beta = 0.4$ , dashed-dotted-dotted line:  $\beta = 0.6$ , big dashed line:  $\beta = 0.8$ ).

Fig. 8 shows the flux of  $\beta$ -meteoroids derived from the impact data. The error given for the flux rate is calculated assuming a Gaussian distribution for the number of impacts. The error in the heliocentric distance presents the range where impact data were considered to derive the respective flux rate. The flux rates are between  $1.5 \cdot 10^{-4} m^{-2} s^{-1}$  at 1.3 AU and  $4.6 \cdot 10^{-6} m^{-2} s^{-1}$  at 2.8 AU whereas a value of about  $9 \cdot 10^{-5} m^{-2} s^{-1}$  is derived for solar ecliptic latitudes between  $67^\circ$  and  $79^\circ$ . The derived flux of  $\beta$ -meteoroids at 1 AU is in agreement with the study of Berg & Grün (1973) which is based on Pioneer data. Our result is also comparable to the interplanetary flux model derived by Grün et al. (1985). The flux of  $\beta$ -meteoroids given in the interplanetary flux model for masses from  $10^{-15}$  to  $10^{-14}$  g reaches a value of about  $8.5 \cdot 10^{-4} m^{-2} s^{-1}$  at 1 AU (The other flux values in the literature for Helios 1 and HEOS 2 refer to the apex flux for larger mass values).

The data indicate a decrease of the detected flux of  $\beta$ -meteoroids at larger solar distances. This can be explained as a result of the radial direction of the flux. A radial direction of the velocity would lead to a  $r^{-2}$ -dependency of the flux rate for the case of constant velocities ( $r$ : solar distance). However,

the velocity changes with solar distance  $r$  and hence the radial dependence of the flux is calculated for different perihelion distances,  $\beta$ -values and eccentricities of the parent body. Fig. 9 shows the variation of the flux rate with the solar distance  $r$ . It is normalized to the flux rate near 1 AU. The derived decrease of the flux rate with solar distance  $r$  is in agreement with the experimental results. Also the higher eccentricity of the orbit of the parent body leads to lower escape velocities and hence  $\beta$ -meteoroids with low  $\beta$ -values. To produce a similar flux rate assuming higher perihelion distances it requires higher  $\beta$ -values compared to the circular orbit. Between 2 and 2.5 AU the enhancement in the flux is probably based on the combined detection of  $\beta$ -meteoroids on prograde and retrograde orbits while the decrease in the data for larger solar distances may indicate a lack of  $\beta$ -meteoroids in retrograde orbits as will be discussed in the next section.

## 7. Selection effects

We discuss some selection effects for the detection probability of the dust detector to estimate this detection probability for particles in prograde respectively retrograde orbits.

Generally objects are moving clockwise or anticlockwise around the Sun. A clockwise moving particle seen from a point in the northern hemisphere (above the ecliptic) is defined as being in retrograde motion, whereas an anticlockwise motion describes a prograde orbit. This property of the orbit is described by the orbital inclination. An inclination within the interval from  $0$  to  $\frac{\pi}{2}$  describes prograde motion, whereas a retrograde orbit contains values of the interval  $(\frac{\pi}{2}, \pi]$ . Taking some geometric consideration into account we make a prediction concerning the motion of the detected particles. The selection effect is influenced by the particular position of Ulysses, Sun and Earth, since the orientation of the spin axis towards the Earth determines the orientation of the detector (see Fig. 10). In the constellation shown in Fig. 10, a predominant detection for particles in retrograde motion is expected. These particles see a larger detection area than particles on prograde orbits, which hit the detector perpendicular to the sensor axis. In this case it is more likely that particles moving retrograde around the Sun impact onto the dust detector, whereas the detection probability for particles which move in the opposite direction is much lower.

A further selection effect mentioned by Wilck (1994) applies to the time dependency of the detection probability of the dust detector within one year. Using constant orbital parameters (inclination and eccentricity) he calculated the effective area for different orbits representing the outgoing (true anomaly  $> 0$ ) and the incoming (true anomaly  $< 0$ ) branch. In his results he shows a periodical change of the detection area with a period of one year. With the help of this result he determined that the months April to July are the favourable period for the detection of  $\beta$ -meteoroids which by definition are on an outgoing branch.

Studying the out-of-ecliptic part of the Ulysses mission only 4 particles can be identified as  $\beta$ -meteoroids in the southern part, 19 particles can be identified as  $\beta$ -meteoroids in the northern part of the orbit. In order to derive the kind of motion the incli-

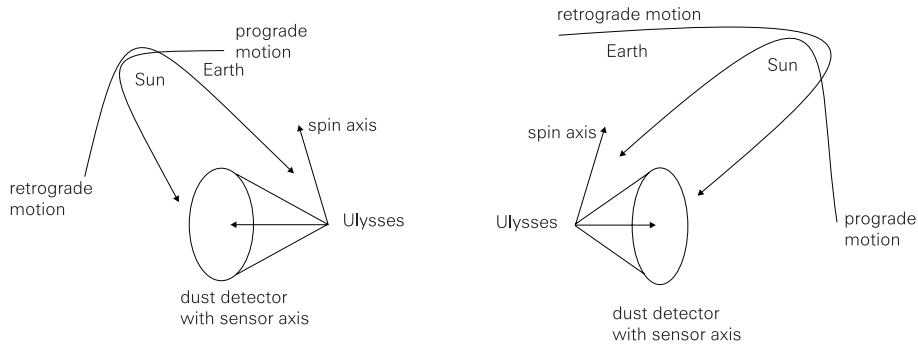


**Fig. 10.** The detection probability is given for prograde (left side) and for retrograde orbits (right side). The particular position of Ulysses, Sun and Earth provides the selection effect accordingly.

nations of these particles are determined. Only the part of the detector, which turns to the Sun, is assumed as a possible impact area to derive the inclination. Out of the 4 particles detected in the southern part 3 are classified to be probably in prograde motion which confirms the geometrical considerations presented before.

From the 19 particles that are identified as  $\beta$ -meteoroids in the northern path, 15 are in prograde orbits and 4 in retrograde. Two of the four retrograde  $\beta$ -meteoroids are detected at the end of the last phase according to the selection effect for retrograde particle. Here, this effect is more distinctive than in the middle of the year where no strong boundary for the selection effect existed. Defining the selection effect which is introduced by Wilck (1994) a little more widely, i.e. from April to the middle of August as the favorable time span, fourteen of the twenty-three noted  $\beta$ -meteoroids confirm this choice. According to this we conclude that  $\beta$ -meteoroids are moving predominantly on prograde orbits, because they are mostly detected when the prograde selection effect applies. Taking into account the influence of the uncertainties of the detector mentioned above we cannot distinguish between prograde and retrograde orbits in the last time interval around the north polar passage, so that the particles in retrograde motion may be as typical as particles with prograde orbits.

## 8. Discussion

Comparing the mass distribution of detected particles to model calculations of  $\beta$ -values as a function of size, we expect the  $\beta$ -meteoroids to have  $\beta$ -values which are larger or equal 0.2. The observed flux rate is then best described with a wide distribution of perihelion distances and the present analysis shows no preference for small perihelion distances. The flux rate of particles that are produced within about 0.1 AU (about 20 solar radii) around the Sun would drop down already in the region beyond 2 AU. This indicates that  $\beta$ -meteoroids identified in the Ulysses data set originate primarily from collisions, because the origin of  $\beta$ -meteoroids by sublimation takes places inside 20 solar radii around the Sun (Mann et al., 1994). As compared to an early analysis by Whipple (1975) we do not assume a certain parent body to be the source of the  $\beta$ -meteoroids, but allow for a variety of initial orbits. Furthermore, the orbital parameters that Whipple used in his analysis are included in the present model assumptions.

Except for the dominance of particles that may be associated with prograde motion we do not see a clear indication for a preference for certain orbital inclinations. The fact that the particles have been detected at high ecliptic latitudes raises the question of whether the particles have been severely influenced by the Lorentz force in their dynamics. The effect of the Lorentz force on small electrically charged dust grains would lead to the ejection of particles from the near solar regions on a wire-like trajectory (Hamilton et al., 1996; Krivov et al., 1998). These models, however, do not allow for a direct comparison, so far, since they do not yield a detailed description of the orbital parameters of the expected fluxes. Hence at this point, we cannot give a clear description of the formation mechanism of the particles. The present result does not show a clear indication for a strong influence of electromagnetic forces: The derived distribution of the perihelion distances does not show a clear peak for very small perihelion distances and the detected  $\beta$ -meteoroids seem to show a majority of particles in prograde motion. The particles detected within the ecliptic have masses which are only slightly smaller than the  $\beta$ -meteoroids identified in the out of ecliptic part, so there is no clear indication that the out-of-ecliptic fluxes are produced by a different effect than the near-ecliptic fluxes.

## 9. Summary

Based on measurements of the dust detector onboard Ulysses, we determine the flux of  $\beta$ -meteoroids to  $1.5 \cdot 10^{-4} m^{-2} s^{-1}$  at solar distances from 1 to 1.6 AU within the ecliptic plane for the first 65 days of the mission. This is in agreement with a previous analysis of the Ulysses measurements within the ecliptic (Baguhl, 1993) and it is also in agreement with other previous measurements (Berg & Grün, 1973). For the out-of-ecliptic part of the mission the flux amounts to  $9 \cdot 10^{-5} m^{-2} s^{-1}$  in the region between 1.8 and 2.7 AU and helioecliptic latitudes between  $67^\circ$  and  $79^\circ$ . The mass distribution of detected  $\beta$ -meteoroids is slightly different from the mass distribution of the (presumably) interplanetary dust component in the data. Taking into account the uncertainties in the speed determination as well as the unreliability in the impact direction a clear distinction between prograde and retrograde motion was not possible for the single impact event. However, from the discussion of the selection effects we can conclude that the detected  $\beta$ -meteoroids are moving predominantly on prograde orbits. As expected from

the flux geometry the flux of  $\beta$ -meteoroids decreases with increasing solar distance. The study of the orbits of particles tends to indicate that the particles are produced at solar distances less than 0.5 AU. However, the present data does not allow for a real determination of the orbital parameters of the particles. We conclude that the main mechanism that has influenced the particles that were identified as  $\beta$ -meteoroids in the Ulysses data set, is most probably the influence of the radiation pressure force. However further studies will be needed to investigate the influence of the solar magnetic field on these small particles.

*Acknowledgements.* The authors are indebted to Eberhard Grün for valuable discussion and advise. This work was supported by BMBF.

## References

- Baguhl M., 1993, Identifikation von Staubeinschlägen in den Daten der Mikrometeoroiden-Detektoren an Bord der Raumsonden Ulysses und Galileo. Dissertation, Max-Planck-Institut für Kernphysik, Heidelberg
- Baguhl M., Grün E., Hamilton D.P., et al., 1994, *Space Sci. Rev.* 72, 471
- Berg O.E., Grün E., 1973, *Space Res.* 13, 1047
- Grün E., Zook H.A., 1980, Dynamics of micrometeoroids. In: Halliday I., McIntosh B.A. (eds.) *Solid Particles in the Solar System*. Proc. IAU Symp. 90, Reidel, Dordrecht, 293
- Grün E., Pailer N., Fechtig H., Kissel J., 1980, *Planet. Space Sci.* 28, 333
- Grün E., Zook H.A., Fechtig H., Giese R.H., 1985, *Icarus* 62, 244
- Grün E., Fechtig H., Giese R.H., et al., 1992a, *ApJS* 92, 411
- Grün E., Fechtig H., Hanner M.S., et al., 1992b, *Space Sci. Rev.*, Ser. 60, 317
- Grün E., Baguhl M., Fechtig H., et al., 1992d, *Geophys. Res. Letters*, 19, 1311
- Grün E., Zook H.A., Baguhl M., et al., 1993, *Nat.* 362, 428
- Grün E., Gustafson B., Mann I., et al., 1994, *A&A* 286, 915
- Grün E., Baguhl M., Divine N., et al., 1995a, *Planet. Space Sci.* 43, 8, 971
- Grün E., Baguhl M., Fechtig H., et al., 1995b, *Planet. Space Sci.* 43, 941
- Grün E., Staubach P., Baguhl M., 1997, *Icarus* 129, 270
- Hamilton D.P., Grün E., Baguhl M., 1996, Electromagnetic escape of dust from the Solar System. In: Gustafson B.Å.S., Hanner M.S. (eds.) *Physics, Chemistry, and Dynamics of Interplanetary Dust*. ASP Conf. Series vol. 104, Kluwer, Dordrecht, p. 31
- Ishimoto H., Mann I., 1996, *Adv. Space Res.* 20, (8), 1523
- Krásak L., 1976, *Bull. Astron. Inst. Czech* 29, 35
- Krivov A., Mann I., Kimura H., 1998, *Earth, Planet and Space* 50, 551
- Krüger H., Grün E., Landgraf M., et al., Three years of Ulysses dust data: 1993 to 1995. *Planet. Space Sci.*, in press
- Leinert C., Röser S., Buitrago J., 1983, *A&A* 118, 345
- Leinert C., Grün E., 1990, Interplanetary Dust, Physics and Chemistry 20, *Space and Solar Physics*. In: Schwenn R., Marsch E. (eds.) *Physics of the Inner Heliosphere, 1. Large-Scale Phenomena*. Springer-Verlag, Berlin, Heidelberg, New York, p. 207
- Mann I., Okamoto H., Mukai T., 1994, *A&A* 291, 1011
- Mukai T., 1985, On the Solar dust ring(s). In: Giese R.H., Lamy P. (eds.) *Properties and Interactions of Interplanetary Dust*. D. Reidel Publishing Company, p. 59
- Mukai T., 1996, Sublimation of Interplanetary Dust. In: Gustafson B.Å.S., Hanner M.S. (eds.) *Physics, Chemistry, and Dynamics of Interplanetary Dust*. ASP Conf. Series vol. 104, Kluwer, Dordrecht, p. 453
- Schwehm G., Rhode M., 1977, *J. Geophys.* 42, 727
- Wenzel K.P., Marsden R.G., Page D.E., Smith E.J., 1992, *ApJS* 92, 207
- Whipple F.L., 1975, Sources of interplanetary dust. In: Elsässer H., Fechtig H. (eds.) *Lecture Notes in Physics 48: Interplanetary Dust and Zodiacal Light*. Springer-Verlag, New York, 403
- Wilck M., 1994, Modellrechnungen zur Auswertung der Ulysses-Staubdaten hinsichtlich der Bahnverteilung und Dynamik in der interplanetaren Staubwolke. Diploma thesis, Univ. Göttingen
- Wilck M., Mann I., 1996, *Planet. Space Sci.* 44, 5, 493
- Witte M., Rosenbauer H., Banaszkiewicz, Fahr H., 1993, *Adv. Space Res.* 13, (6)121
- Zook H.A., Berg O.E., 1975, *Planet. Space Sci.* 23, 183